The dynamics of cortical and hippocampal atrophy in Alzheimer's disease

Mert R. Sabuncu[1,2], PhD; Rahul S. Desikan[1,3], MD, PhD; Jorge Sepulcre[1,4,5], MD, PhD; B.T. Thomas Yeo[1,4], PhD; Hesheng Liu[1], PhD; Nicholas J. Schmansky[1], MSc; Martin Reuter[1], PhD; Michael W. Weiner[7], MD; Randy L. Buckner[1,4,5], PhD; Reisa A. Sperling[1,6] , MD; and Bruce Fischl[1,2], PhD; Alzheimer's Disease Neuroimaging Initiative*

SUPPLEMENTAL MATERIAL

The Cumulative Diffusion Model

Here, we present a mathematical description of the cumulative diffusion model that we used in the present study to describe atrophy. This diffusion process was originally developed to study product adoption mechanisms in markets, cf. [1].

Let us use $N(t)$ to denote the amount of tissue at time t, and $N'(t)$ to denote the (absolute) rate of atrophy (or the negative of the rate of change in the amount of tissue, e.g., measured in mm^3/year). Note $N'(t)$ is a measure of *instantaneous* atrophy, whereas $N(t)$ quantifies the amount of remaining intact tissue. Let t_0 indicate the time at which the degeneration event starts, $N_{\max} = N(t_0)$ be the initial amount of tissue and $N_{\min} = N(+\infty)$ be the final, minimum amount of tissue. Thus $(N_{\max} - N(t))$ is the total amount of atrophy that has occurred so far, and $(N(t) - N_{\min})$ is the amount of tissue to be potentially lost.

The cumulative diffusion model predicts that the rate of atrophy is determined by both the intact tissue and the total amount of atrophy so far, i.e.,

$$N'(t) = b(N_{\max} - N(t))(N(t) - N_{\min}),$$

where b is a negative constant. It is easy to show that the rate of atrophy peaks when $N(t) = (N_{\max} + N_{\min})/2$, i.e., half the potential tissue loss has occurred. This inflection point also marks a shift in dynamics, prior to which atrophy is becoming progressively faster. Beyond this critical point, however, atrophy will be constrained by the amount of intact tissue and thus will gradually slow down.

In the current context, we cannot measure $N_{\max}$ and $N_{\min}$, but we expect them to vary substantially across subjects and across brain regions, since tissue volume is a measurement that is under both genetic and environmental control [2, 3]. One strategy we took in the present study is to use a cognitive performance score (MMSE) as a proxy for disease-specific tissue loss.

The theoretical model we present here should be considered as a partial and simplistic explanation of the underlying complex dynamics. With real data, one would expect to have other mechanisms to play a role, as recognized early on by Bass[1], and in more sophisticated manners that vary over time. Here, our main goal was to present evidence for the cumulative model, which yields a sigmoidal atrophy curve, similar to those recently hypothesized by Jack et al.[4].

CSF Molecular Profile in Cognitively Normal Subjects

Recent converging evidence indicates that cerebrospinal fluid biomarkers of AD, specifically total tau, phosporylated tau and beta-amyloid, are sensitive measurements of AD pathology and abnormal levels of these markers at the individual level are strongly associated with future clinical decline[5, 6]. There is a tight, inverse coupling between brain amyloid deposition (the classical hallmark of AD pathology), as measured in vivo by

Positron Emission Tomography (PET) and the amyloid-binding agent Pittsburgh Compound-B (PIB), and CSF Aβ1-42[7]. In cognitively normal (CN) subjects, CSF Aβ1-42 has been shown to correlate with brain atrophy[8]. In the present study, we employed a recently developed strategy to identify CN individuals with an AD-like CSF profile and who are thus at a high risk of progressing to dementia[9]. Intriguingly, this analysis also suggested that about a third of elderly CN subjects exhibited an AD-like CSF profile, which is also what we observed in our analysis of the ADNI data. This observation is consistent with neuropathological studies on CN subjects[11]. Although this pre-symptomatic group was enriched in APOE-e4 carriers, a well-established genetic risk factor of late-onset AD, the percentage of carriers is significantly less than that of the AD group. Therefore, whether all asymptomatic individuals with abnormal amyloid and/or tau burden will eventually progress to dementia remains an open question that can only be definitely addressed with longitudinal studies that follow CN subjects.

Bias in longitudinal MRI measurements

Our analysis, in particular of the second temporal derivative (i.e., acceleration) of serial MRI measurements is sensitive to potential sources of bias in the longitudinal image processing stream. For example, a systematic bias that results in an over- or under-estimation of the changes in the first time period (e.g., baseline to month 6) relative to the changes in other time periods (e.g. month 6 to month 12) would confound our analysis. FreeSurfer's longitudinal processing pipeline has been designed to specifically address this issue and minimize such bias by treating all the time-points identically and using an unbiased subject-specific template[12]. To examine whether this was in practice the case, we conducted a supplemental analysis on hippocampal and AD-specific cortical atrophy

measurements in the ADNI Cognitively Normal (CN) cohort with at least three MRI scans (N=179). In this group, we have no reason to expect significant differences between the atrophy computed in two subsequent 6-month periods (e.g., baseline - month 6 and month 6 - month 12). Supplemental Figure 1 demonstrates that there is, in fact, no difference between these measurements in the ADNI CN group (paired t-test p-value > 0.5), which indicates that no bias has been introduced by FreeSurfer's longitudinal processing stream.

Atrophy in cognitively normal individuals who progress to MCI/AD

Our analysis of pre-symptomatic individuals suggested that cognitively normal (CN) individuals who are on the trajectory towards clinical AD exhibit a significantly reduced thickness in AD-vulnerable ROIs. On the other hand, hippocampal volume in these subjects is reduced to a lesser extent relative to controls, and the difference was not statistically significant in our analysis. A similar interpretation applies to longitudinal atrophy rates, which our results suggest are statistically indistinguishable from healthy controls and do not track clinical decline during the pre-symptomatic stage. To supplement our analysis of pre-symptomatic individuals, we further examined the ADNI subjects (with at least three MRI scans) who were CN at baseline but converted to MCI/AD over the three years of follow-up (N = 10). Average cortical thickness in AD-vulnerable ROIs and hippocampal volume were both significantly reduced in this pre-symptomatic group ($p < 0.0029$ and $p < 0.021$, respectively), yet the effect size for cortical thickness was larger than hippocampal volume (R square: 0.35 and 0.2, respectively), providing further evidence that the former biomarker is more sensitive than hippocampal volume during the pre-symptomatic stage. Longitudinal rates of atrophy for

AD-vulnerable cortical ROIs and hippocampus in the group of subjects who converted to CN to MCI/AD were also statistically indistinguishable from healthy controls and not correlated with concurrent cognitive decline (p-values > 0.2).

Excluding the entorhinal cortex

The entorhinal cortex, which is part of the medial temporal lobe, is one of the earliest regions targeted in AD. To establish that our characterization of AD-specific thinning was not mainly driven by the entorhinal cortex, we repeated our analysis of baseline and longitudinal changes in average cortical thickness for six AD vulnerable neocortical ROIs that do not include the entorhinal cortex: *inferior parietal sulcus, lateral temporal, inferior parietal, inferior frontal, temporopolar and posterior cingulate cortices*. Supplemental Fig. 2 shows the average baseline thickness and thinning rate in these regions for the different groups. Supplemental Fig. 3 shows the best second-order polynomial fit for the rate of thinning in these six regions as a function of MMSE. The optimum for this curve was at MMSE score 20.7, with a 90% confidence interval of [18.7, 22.6]. These results are consistent with those we obtained by including the entorhinal cortex.

The acceleration/deceleration pattern

The cumulative diffusion model predicts an early acceleration phase followed by a period of deceleration, or slowing down. Our analyses suggested that AD-specific cortical atrophy rates (across the seven ROIs) peak around an MMSE score of [20-23], and rates of hippocampal loss continue to increase until the MMSE score 15. Hence, we hypothesized that longitudinal acceleration (i.e., the second derivative with respect to

time) of cortical thinning is positive for individuals with MMSE score greater than 23, and negative for advanced individuals who have a score less than 20. In contrast, we hypothesized hippocampal atrophy to be speeding up in both groups. The average acceleration patterns for these two biomarkers were in agreement with our hypotheses (see Supp. Figure 4).

To evaluate the statistical significance of the acceleration/deceleration pattern observed for AD-specific cortical thinning, we conducted a permutation test by shuffling the MMSE scores across individuals. For each permutation, we computed and saved the average acceleration in the two groups: the *early* group that consisted of those with an MMSE score greater than 23 and the *advanced* group of those with a score less than 20. These average scores yielded a null distribution for early and late acceleration. The permutation p-value is then computed as the probability (under the null distribution) of observing average acceleration values in the two groups that are more extreme than the true averages. Based on this test, the permutation p-value of the observed average acceleration/deceleration pattern is less than 0.02.

Control region

We conducted a control analysis of the average cortical thickness in pre- and postcentral gyri, which were computed automatically using FreeSurfer's surface parcellation tool[13]. These regions are known to be unaffected during the early stages of AD[14]. Supplemental Fig. 5 shows the average thickness values and thinning rates in these reference regions for three groups: healthy controls (HC), pre-symptomatic individuals with AD-like CSF, and symptomatic (MCI or AD) individuals with AD-like CSF.

Although the average thickness was statistically different between the control group and symptomatic individuals ($p < 0.01$), there was no statistical difference between the control group and pre-symptomatic group. Thinning rates were also indistinguishable between the three groups. Furthermore, thinning rates in these reference ROIs demonstrated no correlation with annual cognitive decline in the group of individuals with an AD-like CSF profile (partial correlation $p > 0.15$).

We further conducted a stepwise regression on the rate of thinning in the pre- and postcentral gyri over the entire group of individuals (pre-symptomatic and symptomatic) with an AD-like CSF profile, with MMSE score (at month 6 follow-up) and its square as independent variables of interest. We included age, sex, education level, APOE-ε4 genotype (1 if ε4 carrier, 0 otherwise), and intra-cranial volume (ICV) as covariates. Neither the MMSE score, nor its square was significantly associated with the thinning rate (p-values > 0.7), thus providing no support for the cumulative diffusion model.

These results confirm that cortical thinning rates in pre- and postcentral gyri do not track disease progression in early AD. However, average thickness values are significantly reduced in the symptomatic group, suggesting that these regions are targeted during later stages.

Supplemental Figure 1

Comparison between atrophy rate measurements obtained with months 0 and 6 versus months 6 and 12. Top: annualized hippocampal volume loss. Bottom: annualized average cortical thinning rate within AD-vulnerable ROIs. For both biomarkers, the two sets of measurements are statistically indistinguishable (paired t-test p-value > 0.5). On each box, the central mark is the median and the edges of the box mark the 25^{th} and 75^{th} percentile in the data. Outliers are indicated with '*'.

Supplemental Figure 2

Left: average cortical thickness in six AD vulnerable neocortical ROIs that do not include the entorhinal cortex across healthy controls (HC); pre-symptomatic and symptomatic (MCI and AD) individuals with AD-like CSF molecular profile. Right: average rates of thinning in these ROIs for each group. Error bars show standard error of the mean. '*' indicates statistically significant ($p < 0.05$) group differences.

Supplemental Figure 3

Scatter plots of rates of AD-specific cortical thinning in six AD vulnerable neocortical ROIs that do not include the entorhinal cortex. Each dot represents an individual with AD-like CSF molecular profile. The green curve represents the best-fit quadratic function. Consistent with the sigmoidal pattern, the curve is concave with an optimum around the MMSE score 20.7.

Supplemental Figure 4

Average acceleration for AD-specific cortical thinning (left) and hippocampal volume loss (right) in two groups of individuals with AD-like CSF molecular profile: (1) with MMSE score greater than 23, and (2) with MMSE score less than 20. Error bars show standard error of the mean.

Supplemental Figure 5

Left: Average cortical thickness in pre- and postcentral gyri across healthy controls (HC); pre-symptomatic and symptomatic (MCI and AD) individuals with AD-like CSF molecular profile. Right: average rates of cortical thinning in these regions for each group. Error bars show standard error of the mean. '*' indicates statistically significant ($p < 0.05$) group difference.

Supplemental Figure 1

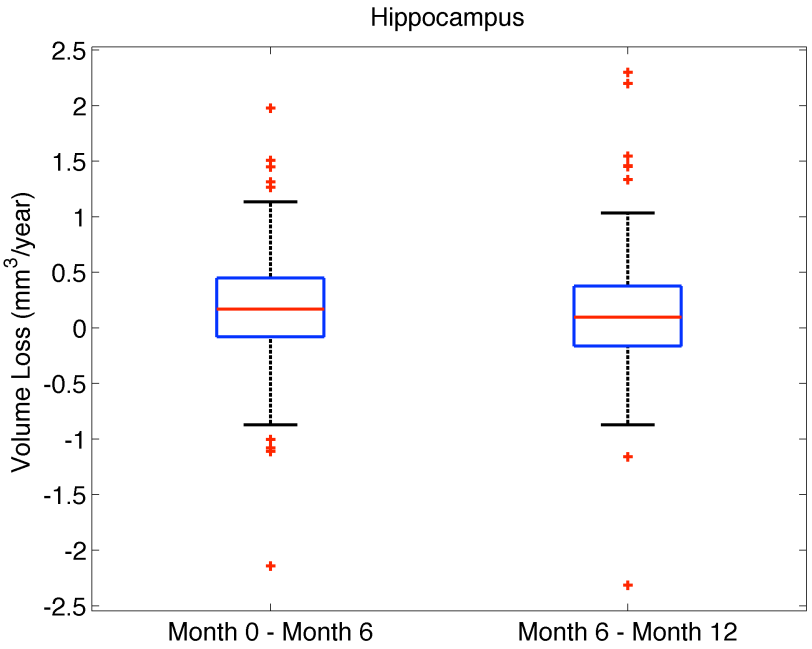

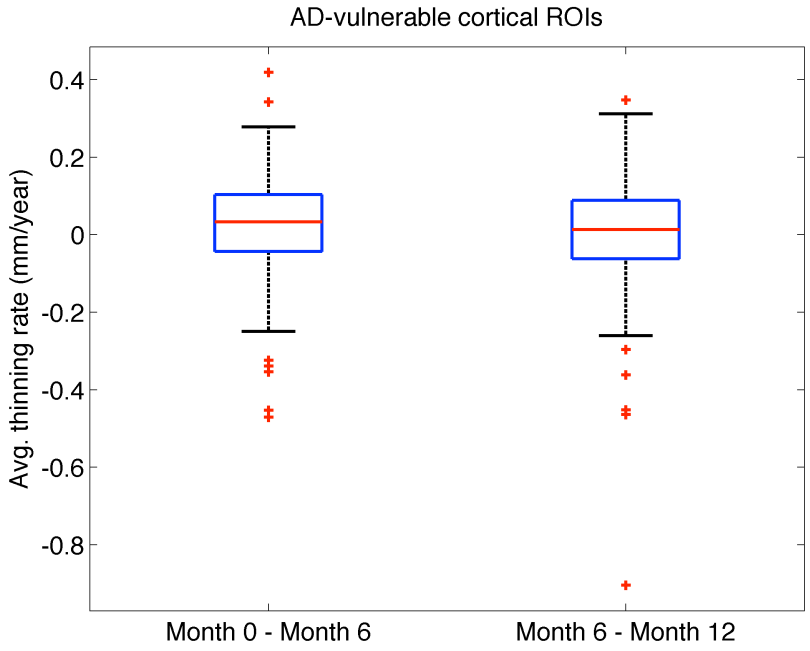

Supplemental Figure 2

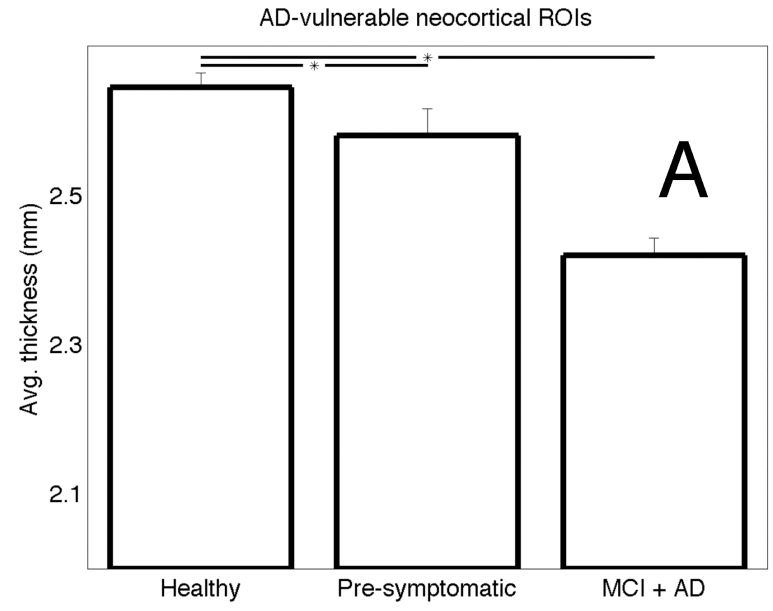

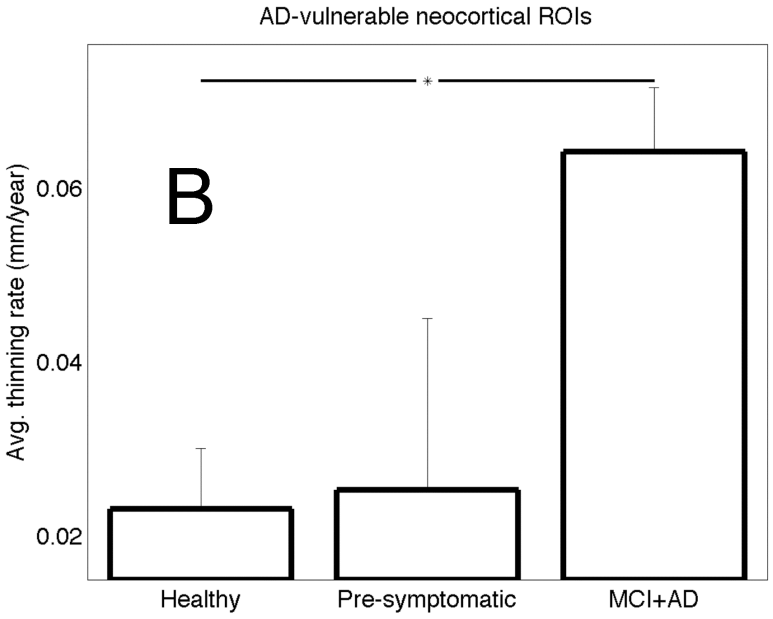

Supplemental Figure 3

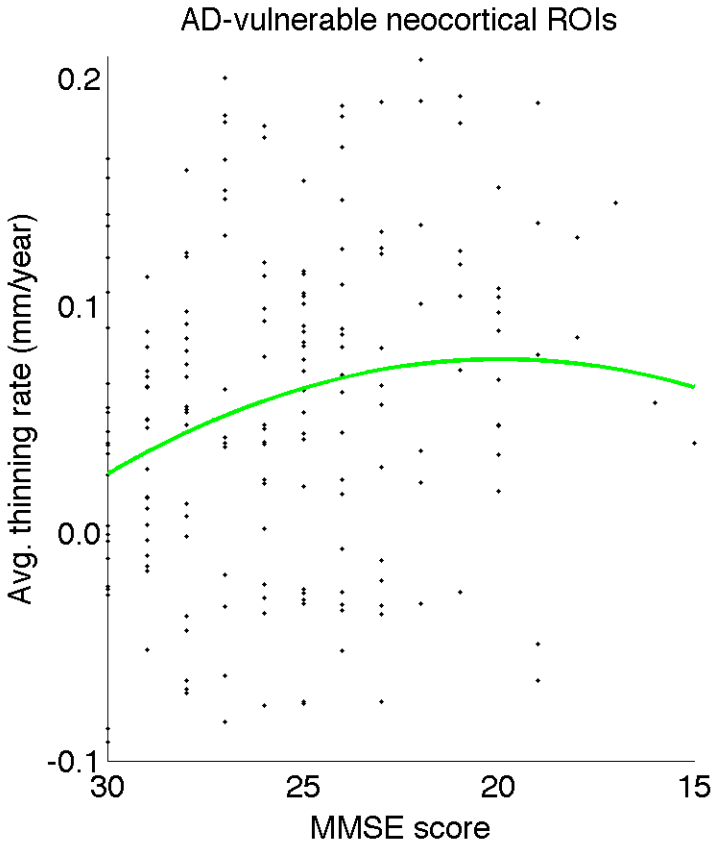

Supplemental Figure 4

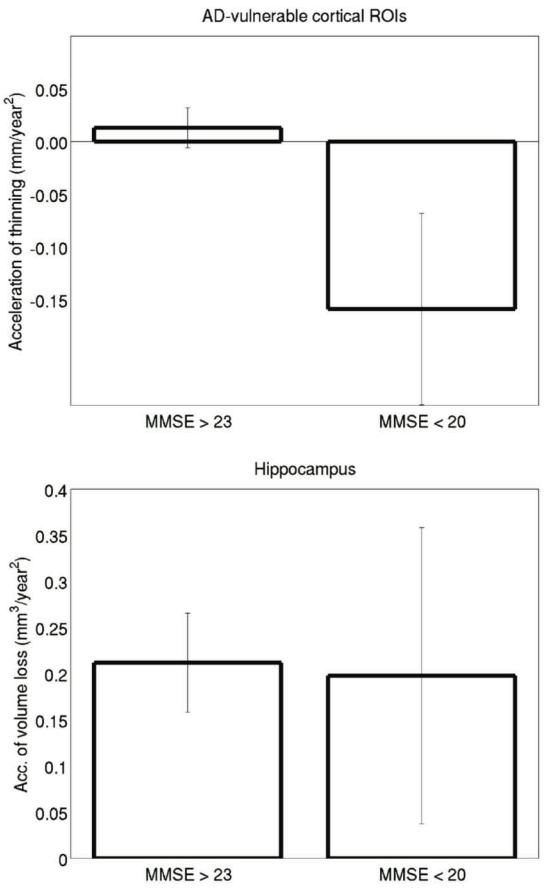

Supplemental Figure 5

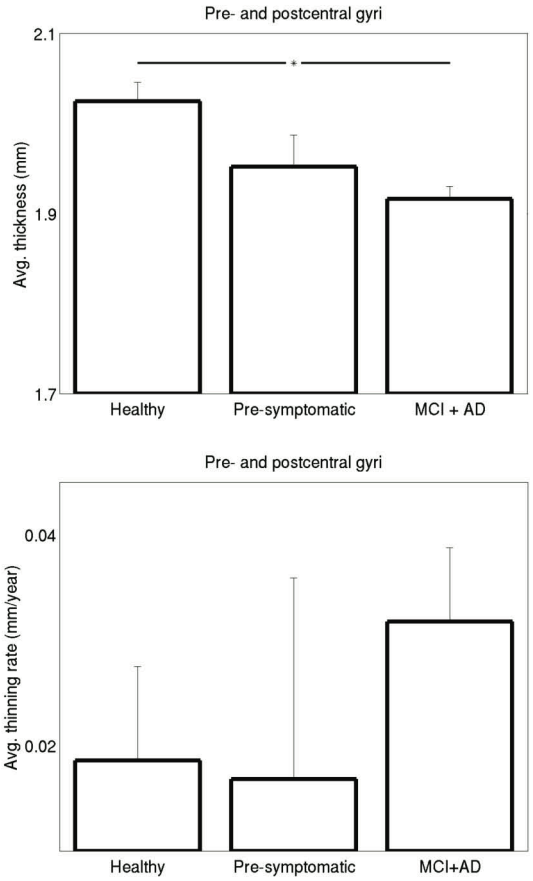

SUPPLEMENTAL TABLES

Supplemental Table I Partial correlation between imaging biomarkers (hippocampal volume, annual hippocampal volume loss, average thickness in AD-vulnerable cortical ROIs, and average thinning rate in AD- vulnerable cortical ROIs) and CSF Aβ1-42 and total tau (continuous) measurements in all cognitive normal subjects (N = 92). Age, sex, education level, APOE-ε4 genotype (1 if ε4 carrier, 0 otherwise), and intra-cranial volume (ICV) were included as covariates. * $p < 0.1$, ** $p < 0.05$

	Hipp. volume	***Hipp. volume loss***	***AD-specific thickness***	***AD-specific thinning***
Total Tau	-0.15	0.05	-0.19*	0.06
ABeta1-42	0.07	-0.17	0.24**	-0.15

Supplemental Table II Partial correlation baseline thickness in seven AD-vulnerable ROIs (IFC: inferior frontal cortex, IPC: inferior parietal cortex, IPS: inferior parietal sulcus, LT: lateral temporal, EC: entorhinal cortex, PCC: posterior cingulate cortex, TP: temporal pole) and CSF Aβ1-42 and total tau (continuous) measurements in all cognitive normal subjects (N = 92). Age, sex, education level, APOE-ε4 genotype (1 if ε4 carrier, 0 otherwise), and intra-cranial volume (ICV) were included as covariates. * $p < 0.1$, ** $p < 0.05$, *** $p < 0.01$

	IFC	***IPC***	***IPS***	***LT***	***EC***	***PCC***	***TP***
Total Tau	0.01	-0.27**	-0.01	-0.21**	-0.01	-0.05	-0.21*
ABeta1-42	0.11	0.26**	0.13	0.05	0.01	0.31***	0.15

Supplemental Table III The MMSE scores at which annual thinning rates in seven AD-vulnerable ROIs peak. (IFC: inferior frontal cortex, IPC: inferior parietal cortex, IPS: inferior parietal sulcus, LT: lateral temporal, EC: entorhinal cortex, PCC: posterior cingulate cortex, TP: temporal pole). 95% confidence intervals are listed in square brackets.

IFC	***IPC***	***IPS***	***LT***	***EC***	***PCC***	***TP***
24.1	24.2	24.3	23.8	24.0	24.4	22.7
[22.2-26.0]	[22.3-26.1]	[22.5-26.3]	[21.9-25.7]	[22.2-26.0]	[22.5-26.3]	[20.8-24.6]

SUPPLEMENTAL REFERENCES

1. Bass F. Comments on" A New Product Growth for Model Consumer Durables": The Bass Model. Management science. 2004:1833-40.

2. Panizzon M, Fennema-Notestine C, Eyler L, et al. Distinct genetic influences on cortical surface area and cortical thickness. Cerebral Cortex. 2009.

3. Lazar S, Kerr C, Wasserman R, et al. Meditation experience is associated with increased cortical thickness. Neuroreport. 2005;16(17):1893.

4. Jack Jr C, Knopman D, Jagust W, et al. Hypothetical model of dynamic biomarkers of the Alzheimer's pathological cascade. The Lancet Neurology. 2010;9(1):119-28.

5. Blennow K, Hampel H, Weiner M, Zetterberg H. Cerebrospinal fluid and plasma biomarkers in Alzheimer disease. Nature Reviews Neurology. 2010;6(3):131-44.

6. Fagan A, Roe C, Xiong C, Mintun M, Morris J, Holtzman D. Cerebrospinal fluid tau/beta-amyloid42 ratio as a prediction of cognitive decline in nondemented older adults. Archives of neurology. 2007:64.3.

7. Fagan A, Mintun M, Mach R, et al. Inverse relation between in vivo amyloid imaging load and cerebrospinal fluid A 42 in humans. Annals of neurology. 2006;59(3):512-9.

8. Fagan A, Head D, Shah A, et al. Decreased cerebrospinal fluid A 42 correlates with brain atrophy in cognitively normal elderly. Annals of neurology. 2009;65(2):176-83.

9. Shaw L, Vanderstichele H, Knapik-Czajka M, et al. Cerebrospinal fluid biomarker signature in Alzheimerís disease neuroimaging initiative subjects. Annals of neurology. 2009;65(4):403.

10. Meyer GD, Shapiro F, Vanderstichele H, et al. Diagnosis-Independent Alzheimer Disease Biomarker Signature in Cognitively Normal Elderly People. Archives of Neurology. 2010;67(8):949-56.

11. Davis D, Schmitt F, Wekstein D, Markesbery W. Alzheimer neuropathologic alterations in aged cognitively normal subjects. Journal of Neuropathology & Experimental Neurology. 1999;58(4):376.

12. Reuter M, Rosas H, Fischl B. Highly accurate inverse consistent registration: A robust approach. Neuroimage. 2010 December 2010;53(4):1181-96.

13. Desikan R, SÈgonne F, Fischl B, et al. An automated labeling system for subdividing the human cerebral cortex on MRI scans into gyral based regions of interest. Neuroimage. 2006;31(3):968-80.

14. Dickerson B, Bakkour A, Salat D, et al. The cortical signature of Alzheimer's disease: regionally specific cortical thinning relates to symptom severity in very mild to mild AD dementia and is detectable in asymptomatic amyloid-positive individuals. Cerebral Cortex. 2009;19(3):497.